

Preparation, Structure Characterization, and Oxidation Activity of Ruthenium Complexes with Tripodal Ligands Bearing Noncovalent Interaction Sites

Koichiro Jitsukawa,* Yoshiyuki Oka, Syuhei Yamaguchi, and Hideki Masuda*

Department of Applied Chemistry, Graduate School of Engineering,
Nagoya Institute of Technology, Showa-ku, Nagoya 466-8555, Japan

Received April 30, 2004

Ruthenium(II/III) complexes with tripodal tris(pyridylmethyl)amine ligands bearing one, two, or three pivalamide groups (MPPA, BPPA, TPPA: amide-series ligands) or neopentylamine ones (MNPA, BNPA, TNPA: amine-series ligands) at the 6-position of the pyridine ring have been synthesized and structurally characterized. The X-ray structure analyses of the single crystals of these complexes reveal that they complete an octahedral geometry with the tripodal ligand and some monodentate ligands. The amide-series ligands prefer to form a Ru(II) complex, while the amine-series ones give a Ru(III) complex. In the presence of PhIO oxidant, the catalytic activities for epoxidation of olefins, hydroxylation of alkane, and dehydrogenation of alcohol have been investigated using the six ruthenium complexes [Ru^{II}(tppa)Cl₂] (1), [Ru^{III}(tnpa)Cl₂]PF₆ (2), [Ru^{II}(bppa)Cl]PF₆ (3), [Ru^{III}(bnpa)Cl₂]PF₆ (4), [Ru^{II}(mppa)Cl]PF₆ (5), and [Ru^{III}(mnpa)Cl₂]PF₆ (6). Among them, the amide-series complexes, 1, 3, and 5, showed a higher epoxidation activity in comparison with the amine-series ones, 2, 4, and 6. On the other hand, the latter showed a higher reactivity for hydroxylation, allylic oxidation, and C=C bond cleavage reactions compared with the former. Such a complementary reactivity is interpreted by the character of the ruthenium–oxo species involving electronically equivalent formulas, Ru(V)=O and Ru(IV)–O[•].

Introduction

High-valent metal–oxo species have been proposed as one of the active intermediates not only in biological metalloenzymes such as oxidases and oxygenases but also in the oxidative transformation of organic compounds catalyzed by transition metal complexes.^{1–4} In enzyme reactions catalyzed by a heme protein, a high-valent iron–oxo intermediate plays an important role for an oxidative transformation of a biorelated compound.⁵ In non-heme enzymes, such an iron–oxo species has been also postulated as an active intermediate by some researchers.^{6–9} Recently, an Fe(IV)=O species has

been characterized structurally using a non-heme model complex with a bulky ligand.¹⁰ Fe=O species, however, have rarely been characterized because of their labilities.¹¹ Therefore, ruthenium(IV, V, or VI)–oxo species, which are generated from the reaction of low-valent ruthenium(II or III) complexes and various oxidants, are widely utilized as catalysts for oxygen transfer reactions,^{12–18} because the ruthenium complexes are often employed as a stable homologous

* Authors to whom correspondence should be addressed. E-mail: jitsukawa.koichiro@nitech.ac.jp (K.J.), masuda.hideki@nitech.ac.jp (H.M.).

- Holm, R. H. *Chem. Rev.* **1987**, *87*, 1401.
- Ostovic, D.; Bruce, T. C. *Acc. Chem. Res.* **1992**, *25*, 314.
- Meunier, B. *Chem. Rev.* **1992**, *92*, 1411.
- Mayer, J. M. *Acc. Chem. Res.* **1998**, *31*, 441.
- Cytochrome P-450: Structure, Mechanism and Biochemistry*, 2nd ed.; Ortiz de Montellano, P. R., Ed.; Plenum Press: New York, 1995.
- Shu, L.; Nesheim, J. C.; Kauffmann, K.; Munck, E.; Lipscomb, J. D.; Que, L., Jr. *Science* **1997**, *275*, 515.
- Valegard, K.; Terwisscha van Scheltinga, A. C.; Lloyd, M. D.; Hara, T.; Ramaswamy, S.; Perrakis, A.; Thompson, A.; Lee, H.-J.; Baldwin, J. E.; Schofield, C. J.; Hajdu, J.; Anderson, I. *Nature* **1998**, *394*, 805.

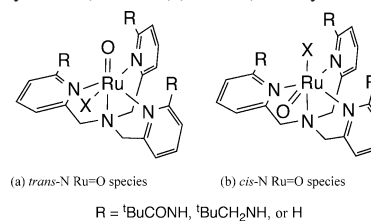
- Liu, P.; Murakami, K.; Seki, T.; He, X.; Yeung, S.-M.; Kuzuyama, T.; Seto, H.; Liu, H.-W. *J. Am. Chem. Soc.* **2001**, *123*, 4619.
- Liu, A.; Ho, R. Y. N.; Que, L., Jr.; Ryle, M. J.; Phinney, B. S.; Hausinger, R. P. *J. Am. Chem. Soc.* **2001**, *123*, 5126.
- Rohde, J.-U.; In, J.-H.; Lim, M. H.; Brennessel, W. W.; Bukowski, M. R.; Stubna, A.; Munck, E.; Nam, W.; Que, L., Jr. *Science* **2003**, *299*, 1037.
- Lim, M. H.; Rohde, J.-U.; Stubna, A.; Bukowski, M. R.; Costas, M.; Ho, R. Y. N.; Munck, E.; Nam, W.; Que, L., Jr. *Proc. Natl. Acad. Sci. U.S.A.* **2003**, *100*, 3665.
- Che, C.-M.; Yam, V. W.-W. *Adv. Inorg. Chem.* **1992**, *39*, 233.
- Griffith, W. P. *Chem. Soc. Rev.* **1992**, *179*.
- Naota, T.; Takaya, H.; Murahashi, S.-I. *Chem. Rev.* **1998**, *98*, 2599.
- Fung, W.-H.; Yu, W.-Y.; Che, C.-M. *J. Org. Chem.* **1998**, *63*, 7715.
- Groves, J. T.; Quinn, R. J. *Am. Chem. Soc.* **1985**, *107*, 5790.
- Lai, T.-S.; Zhang, R.; Cheung, K.-K.; Kwong, H.-L.; Che, C.-M. *Chem. Commun.* **1998**, 1583.
- Neumann, R.; Dahan, M. *J. Am. Chem. Soc.* **1998**, *120*, 11969.

element in the place of iron. To characterize mononuclear Ru=O species, some ruthenium complexes with tripodal polypyridine derivatives have been studied previously.^{19–21} We have also indicated that the tripodal ligands with substituent groups at the pyridine 6-position contribute to the stabilization of the axial ligand through hydrogen bonds, steric factors, and electrostatic effects around the coordination sphere.^{22–28}

In the ruthenium-catalyzed oxidations, iodosobenzene (PhIO) is sometimes utilized as an efficient 2-electron oxidant for generation of Ru=O species to avoid complicated oxidation pathways.^{1,12–15,29–39} Previously, we have reported that some ruthenium complexes with tripodal tris(2-pyridylmethyl)amine (TPA) derivatives catalyzed hydroxylation of adamantane and epoxidation of cyclohexene in the presence of PhIO, in which the complementarity between hydroxylation and epoxidation was observed in the ruthenium complexes containing electron-withdrawing substituents or electron-donating ones at the pyridine 6-position of TPA.⁴⁰ The character of the ruthenium-oxo species (Ru(V)=O) controlled by the 6-substituent groups affected the reactivities for hydroxylation and epoxidation. Such complementary reactivity might be caused by two kinds of oxo species, trans-N(tertiary amine) and cis-N(tertiary amine) Ru=O species as illustrated in Chart 1. We consider that these two species operate concurrently during the reaction.

It is known that the catalytic activity of cytochrome P-450 is affected by the axially coordinated proximal ligand at the trans position to metal-oxo species (trans influence).^{5,41}

Chart 1. Ruthenium–Oxo Complexes with Tripodal Ligands: (a) Trans-N(Tertiary Amine) Form; (b) Cis-N(Tertiary Amine) Form



Hence, taking into account the trans influence, we also succeeded in controlling the catalytic activity of the metal-oxo species with a square-planar aromatic ligand when a monodentate axial ligand coordinated to its trans position was used.⁴² To clarify the character of ruthenium-oxo species, we have investigated the correlation of the structural diversity of the complexes and the catalytic activities. Here, we describe the preparation of ruthenium-oxo species, of which catalytic activity is controlled by the tripodal tris(2-pyridylmethyl)amine ligands bearing one, two, and three pivalamide groups (MPPA, BPPA, TPPA: amide-series ligands) or neopentylamine groups (MNPA, BNPA, TNPA: amine-series ligands) at the pyridine 6-position (Chart 2). In these substituent groups, the 6-neopentylamino group is classified as an electron-donating one and the 6-pivalamide one is an electron-withdrawing pivalamide one.^{43,44}

Experimental Section

Materials and Measurements. Reagents used for synthesis were the highest grade available, which were employed without further purification. All solvents for spectroscopic measurements were purified by distillation before use.

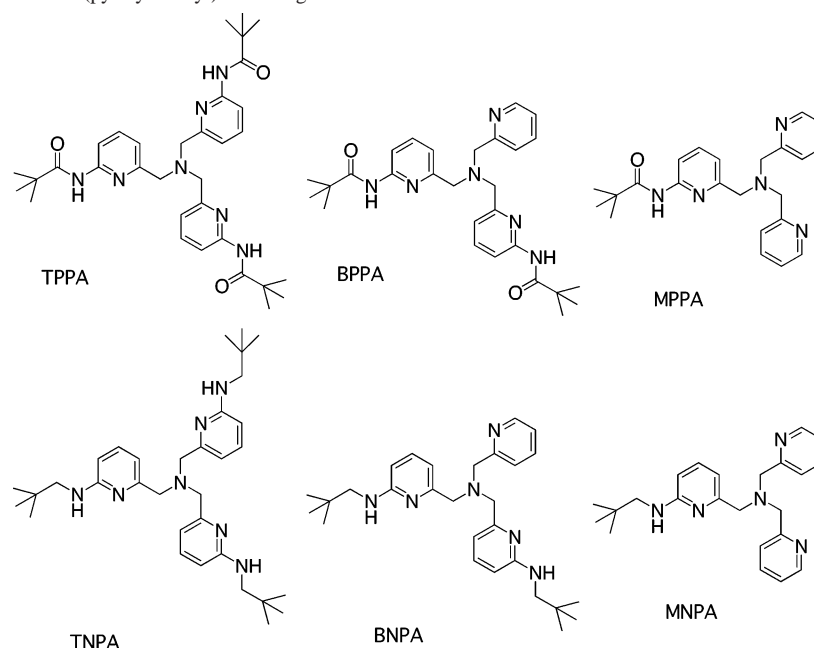
Electronic absorption spectra were recorded on JASCO UVIDECE-660. ¹H NMR spectra were measured on a Varian VXR-300S or JEOL Lambda-500 spectrometer with TMS as an internal standard. GC analysis with an internal standard method for oxidation products was performed by use of Shimadzu GC8F apparatus equipped with a PEG-20M or silicon OV-17 column. ESI mass spectra for characterization of Ru=O species in dichloromethane solution were taken with a JEOL JMS-700 or Micromass LCT. IR spectra measured with a KBr pellet were performed by use of a JASCO FT/IR-410.

Single crystals of **1**, **2a**, **3–5**, **8**, and **9** suitable for X-ray diffraction measurements were obtained from the corresponding solutions standing several days at room temperature. The crystals were mounted on a glass capillary, and the diffraction data were collected on various X-ray instruments as below. Crystallographic and diffraction data were obtained as below: **1**, **4**, and **9**, a Rigaku RAXIS-IV imaging plate area detector using graphite-monochromated Mo K α radiation; **2a**, **3**, **5**, and **8**, Enraf-Nonius CAD4-EXPRESS four-circle diffractometer with graphite-monochromated Mo K α radiation. The crystallographic data and experimental details are listed in Table 1. In the crystal of **9**, there were two independent molecules in the unit cell. All the structures were solved by a combination of direct methods and Fourier techniques. Non-

- (19) Che, C.-M.; Yam, V. W.-W.; Mak, T. C. *J. Am. Chem. Soc.* **1990**, *112*, 2284.
 (20) Kojima, T. *Chem. Lett.* **1996**, 121.
 (21) Yamaguchi, M.; Kousaka, H.; Yamagishi, T. *Chem. Lett.* **1997**, 769.
 (22) Harata, M.; Jitsukawa, K.; Masuda, H.; Einaga, H. *J. Am. Chem. Soc.* **1994**, *116*, 10817.
 (23) Harata, M.; Jitsukawa, K.; Masuda, H.; Einaga, H. *Chem. Lett.* **1995**, 61.
 (24) Harata, M.; Jitsukawa, K.; Masuda, H.; Einaga, H. *Bull. Chem. Soc. Jpn.* **1998**, *71*, 637.
 (25) Wada, A.; Harata, M.; Hasegawa, K.; Jitsukawa, K.; Masuda, H.; Mukai, M.; Kitagawa, T.; Einaga, H. *Angew. Chem., Int. Ed.* **1998**, *37*, 798.
 (26) Harata, M.; Hasegawa, K.; Jitsukawa, K.; Masuda, H.; Einaga, H. *Bull. Chem. Soc. Jpn.* **1998**, *71*, 1031.
 (27) Wada, A.; Ogo, S.; Watanabe, Y.; Mukai, M.; Kitagawa, T.; Jitsukawa, K.; Masuda, H.; Einaga, H. *Inorg. Chem.* **1999**, *38*, 3592.
 (28) Wada, A.; Ogo, S.; Nagatomo, S.; Kitagawa, T.; Watanabe, Y.; Jitsukawa, K.; Masuda, H. *Inorg. Chem.* **2002**, *41*, 616.
 (29) Hudlicky, M. *Oxidations in Organic Chemistry*; ACS Monograph 186; American Chemical Society: Washington, DC, 1990.
 (30) Murahashi, S.-I.; Komiya, N.; Oda, Y.; Kuwabara, T.; Naota, T. *J. Org. Chem.* **2000**, *65*, 9186.
 (31) Braf G. A.; Sheldon, R. A. *J. Mol. Catal. A: Chem.* **1995**, *102*, 23.
 (32) Che, C.-M.; Ho, C.; Lau, T.-C. *J. Chem. Soc., Dalton Trans.* **1991**, 1259.
 (33) Stultz, L. K.; Binstead, R. A.; Reynolds, M. S.; Meyer, T. J. *J. Am. Chem. Soc.* **1995**, *117*, 2520.
 (34) Gross, Z.; Ini, S. *J. Org. Chem.* **1997**, *62*, 5514.
 (35) Lai, T.-S.; Kwong, H.-L.; Zhang, R.; Che, C.-M. *J. Chem. Soc., Dalton Trans.* **1998**, 3559.
 (36) Catalano, V. C.; Heck, R. A.; Immoos, C. E.; Ohaman, A.; Hill, M. G. *Inorg. Chem.* **1998**, *37*, 2150.
 (37) Fung, W.-H.; Yu, W.-Y.; Che, C.-M. *J. Org. Chem.* **1998**, *63*, 7715.
 (38) Lebeau, E. L.; Meyer, T. J. *Inorg. Chem.* **1999**, *38*, 2174.
 (39) Liu, C.-J.; Yu, W.-Y.; Che, C.-M.; Yeung, C.-H. *J. Org. Chem.* **1999**, *64*, 7365.
 (40) Jitsukawa, K.; Oka, Y.; Einaga, H.; Masuda, H. *Tetrahedron Lett.* **2001**, *42*, 3467.

- (41) Auclair, K.; Moenne-Loccoz, P.; Ortiz de Montellano, P. R. *J. Am. Chem. Soc.* **2001**, *123*, 4877 and references therein.
 (42) Jitsukawa, K.; Shiozaki, H.; Masuda, H. *Tetrahedron Lett.* **2002**, *43*, 1491.
 (43) Jones, R. A.; Katritzky, A. R. *J. Chem. Soc.* **1959**, 1317.
 (44) Rasala, D. *Bull. Soc. Chim. Fr.* **1992**, *129*, 79.

Chart 2. Tripodal 6-Substituted Tris(pyridylmethyl)amine Ligands



hydrogen atoms are anisotropically refined by full-matrix least-squares calculations. Hydrogen atoms were included but not refined. Atomic scattering factors and anomalous dispersion terms were taken from ref 45. All the calculations were carried out on a Japan SGI workstation computer using the teXsan crystallographic software package.⁴⁶

Preparation of Ligands. Tripodal ligands (Chart 2), TPPA, TNPA, BPPA, BNPA, MPPA, and MNPA, were synthesized according to the previously reported method.^{22–28,47} The structures of all ligands employed here were confirmed by the elemental and ¹H NMR analyses.

Abbreviations: tris((6-pivalamide-2-pyridyl)methyl)amine (TPPA); tris(6-((neopentylamino)-2-pyridyl)methyl)amine (TNPA); bis(6-(pivalamide-2-pyridyl)methyl)(2-pyridylmethyl)amine (BPPA); bis(6-(neopentylamino)-2-pyridyl)methyl(2-pyridylmethyl)amine (BNPA); ((6-pivalamide-2-pyridyl)methyl)bis(2-pyridylmethyl)amine (MPPA); ((6-neopentylamino)-2-pyridyl)methylbis(2-pyridylmethyl)amine (MNPA); tris(2-pyridylmethyl)amine (TPA).

Synthesis and Characterization of Ruthenium Complexes. Syntheses of the ruthenium(III) complexes were carried out under nitrogen atmosphere in refluxing EtOH solution containing RuCl₃·3H₂O and the tripodal ligand prepared as above.⁴⁸ Syntheses of ruthenium(II) complexes were also carried out with addition of Et₃N to the above ethanol solution under nitrogen atmosphere.⁴⁹ The reference complex, [Ru(tpa)Cl₂]ClO₄ (**7a**), was prepared according to the reported method.⁴⁸ The Ru(III)–OH complex, [Ru^{III}(tnpa)-(OH)Cl]CF₃SO₃ (**9**), was prepared from the reaction of AgCF₃SO₃ and the [Ru^{III}(tnpa)Cl₂]Cl (**2b**) in aqueous acetone solution.^{50,51} All ruthenium(II or III) complexes employed here except the MNPA

complex were obtained as a single crystal suitable for X-ray analysis. The preparation methods and spectral and elemental analysis data for the complexes are shown below:

[Ru^{II}(tpa)Cl₂] (1**).** A solution of RuCl₃·3H₂O (50 mg, 0.2 mmol) and TPPA (112 mg, 0.19 mmol) in EtOH (30 mL) was refluxed for 1 h under nitrogen atmosphere, and then Et₃N (24 mg, 0.24 mmol) was added to the solution. The color of the solution changed from dark brown to clear red with addition of Et₃N. After 24 h, the reaction solution was filtered and then evaporated to a 3 mL volume. The condensed solution was allowed to stand in a refrigerator for several days. A dark red complex, **1** (98 mg), was precipitated as a single crystal suitable for X-ray analysis. The isolated yield of **1**, based on the starting RuCl₃·3H₂O, was 65%.

The absorption spectrum of **1** in dichloromethane solution exhibited absorption maxima at 436 nm ($\epsilon = 7200 \text{ M}^{-1} \text{ cm}^{-1}$) and 371 nm ($\epsilon = 5700 \text{ M}^{-1} \text{ cm}^{-1}$) assignable to MLCT ($d \rightarrow \pi^*$) transitions. The ESI-mass spectral data were not obtained, because this complex was hardly ionized in the mass analysis. Anal. Calcd for **1** (C₃₃H₄₅Cl₂N₇O₃Ru·C₂H₅OH): C, 52.16; H, 6.38; N, 12.16. Found: C, 52.08; H, 6.17; N, 12.04. ¹H NMR (DMSO-*d*₆): $\delta = 9.5\text{--}11.5$ (bs, 3H), 7.0–8.2 (m, 9H), 4.0–4.9 (m, 6H), 1.2–1.4 (bs, 27H).

[Ru^{III}(tnpa)Cl₂]Cl (2b**).** A solution of RuCl₃·3H₂O (50 mg, 0.2 mmol) and TNPA (105 mg, 0.19 mmol) in EtOH (30 mL) was refluxed under nitrogen atmosphere for 24 h. The color of the solution changed from dark brown to clear green during the progress of the reaction. After filtration and evaporation, the residue was dissolved in chloroform. Addition of diethyl ether to the chloroform solution gave a 128 mg (85%) of crude precipitate **2b**.

[Ru^{III}(tnpa)Cl₂]PF₆ (2**) and [Ru^{III}(tnpa)Cl₂]ClO₄ (**2a**).** To a dichloromethane–MeOH (1:1) solution of the crude **2b** was added an aqueous solution of NaPF₆ (37 mg, 0.22 mmol) or NaClO₄ (27 mg, 0.22 mmol). After the solution was standing at room temperature for several days, crystals of **2** or **2a** precipitated. A single crystal of a green complex, [Ru^{III}(tnpa)Cl₂]ClO₄ (**2a**), was suitable for X-ray study.

(45) *International Tables for X-ray Crystallography*; Ibers, J. A., Hamilton, W. C., Ed.; Kynoch Press: Birmingham, U.K., 1974; Vol. IV.

(46) *teXsan, Crystal Structure Analysis Package*; Molecular Structure Corp.: The Woodlands, TX, 1992.

(47) Ogo, S.; Wada, S.; Watanabe, Y.; Iwase, M.; Wada, A.; Harata, M.; Jitsukawa, K.; Masuda, H.; Einaga, H. *Angew. Chem., Int. Ed.* **1998**, *37*, 2102.

(48) Kojima, T.; Amano, T.; Ishii, Y.; Ohba, M.; Okae, Y.; Matsuda, Y. *Inorg. Chem.* **1998**, *37*, 4076.

(49) Kojima, T.; Tsuchida, J.; Nakashima, S.; Ohya-Nishiguchi, H.; Yano, S.; Hidai, M. *Inorg. Chem.* **1992**, *31*, 2333.

(50) Liobet, A.; Doppelt, P.; Meyer, T. J. *Inorg. Chem.* **1988**, *27*, 514.

(51) Ho, C.; Che, C.-M.; Lau, T.-C. *J. Chem. Soc., Dalton Trans.* **1990**, 967.

Table 1. Crystallographic Data and Experimental Details for the Ruthenium Complexes

param	[Ru(tppa)Cl ₂]-C ₂ H ₅ OH (1)	[Ru(tppa)Cl ₂]-C ₂ H ₅ OH (2a)	[Ru(bppa)Cl ₂]-PF ₆ -CH ₃ OH (3)	[Ru(bnpa)Cl ₂]-PF ₆ -H ₂ O (4)	[Ru(mppa)Cl]PF ₆ (5)	[Ru(tppa)Cl ₃] (8)	{[Ru(tnpa)(OH)Cl](CF ₃ SO ₃) ₂] (9)
formula	C ₃₃ H ₅₁ Cl ₂ N ₇ O ₄ Ru	C ₃₃ H ₅₇ Cl ₃ N ₇ O ₄ Ru	C ₂₉ H ₄₀ ClF ₆ N ₆ O ₃ PRu	C ₂₈ H ₄₂ Cl ₂ F ₆ N ₆ OPRu	C ₂₃ H ₂₇ ClF ₆ N ₅ OPRu	C ₃₃ H ₄₅ Cl ₃ N ₇ O ₃ Ru	C ₆₈ H ₁₀₄ Cl ₂ F ₆ N ₁₄ O ₈ Ru ₂ S ₂
fw	805.81	871.28	802.16	795.62	670.99	795.19	1696.82
cryst color	dark red	green	dark red	green	orange	orange	blue
cryst system	monoclinic	monoclinic	triclinic	monoclinic	monoclinic	monoclinic	monoclinic
space group	P2 ₁ /c (No. 14)	P2 ₁ /c (No. 14)	P1 (No. 2)	P2 ₁ (No. 4)	P2 ₁ (No. 4)	Cc (No. 9)	Cc (No. 9)
a, Å	16.858(2)	11.317(2)	11.048(7)	8.697(3)	8.930(2)	9.203(7)	22.457(4)
b, Å	11.704(1)	16.462(2)	13.137(2)	16.353(3)	11.658(2)	32.344(1)	23.066(6)
c, Å	21.433(1)	23.769(2)	13.427(2)	12.652(4)	13.548(2)	13.077(7)	16.692(2)
α, deg			80.17(8)				
β, deg			88.29(8)	102.78(2)	107.59(2)	94.39(1)	95.99(1)
γ, deg			75.47(4)				
V, Å ³			1858(1)	1754.8(9)	1344.5(5)	3881(3)	8599(2)
Z	4	4	2	2	2	4	4
ρ _{calcd} , g cm ⁻³	1.349	1.336	1.433	1.506	1.657	1.361	1.311
μ, cm ⁻¹	5.74	5.96	6.04	7.08	8.10	6.51	5.30
R ₁ ^a	0.051	0.092	0.083	0.084	0.038	0.060	0.063
R _w ^b	0.147	0.212	0.257	0.217	0.096	0.145	0.175
λ, Å	0.7107	0.7109	0.7107	0.7107	0.7107	0.7107	0.7107
data/obsd	7091	7066	7540	2761	2895	3963	7051
data/used	6831	2693	3413	1971	2625	2401	6214
GOF	1.072	2.241	1.148	1.056	1.403	1.283	1.064
temp, K	288	273	273	288	273	273	288

$$^a R_1 = \sum ||F_o| - |F_c|| / \sum |F_o| \quad ^b R_w = [\sum w(F_o - F_c)^2 / \sum w(F_c)^2]^{1/2}; \quad w = 4F_o^2 / \sigma^2(F_o)^2.$$

The absorption spectra of **2** and **2a,b** in dichloromethane solution showed absorption maxima at 694 nm ($\epsilon = 1700 \text{ M}^{-1} \text{ cm}^{-1}$) and 324 nm ($\epsilon = 12300 \text{ M}^{-1} \text{ cm}^{-1}$) assignable to MLCT bands. The ESI-mass spectrum gave prominent peak clusters at $m/z = 717.8$ corresponding to $[\text{Ru}^{\text{III}}(\text{tnpa})\text{Cl}_2]^+$. Any spectral differences were not observed among the complexes of **2** and **2a,b**. Anal. Calcd for **2** (C₃₃H₅₁Cl₂F₆N₇PRu): C, 45.96; H, 5.96; N, 11.36. Found: C, 46.31; H, 5.81; N, 11.33.

[Ru^{II}(bppa)Cl]PF₆ (3). A solution of RuCl₃·3H₂O (50 mg, 0.2 mmol) and BPPA (91 mg, 0.19 mmol) in MeOH (30 mL) was refluxed for 1 h under nitrogen atmosphere, and then Et₃N (24 mg, 0.24 mmol) was added to the solution. After 18 h of reaction under a nitrogen atmosphere, the reaction solution was filtered and then evaporated to 3 mL volume, to which addition of acetone gave crude [Ru(bppa)Cl]Cl complex. This was dissolved in dichloromethane–MeOH solution under nitrogen atmosphere, to which addition of NaPF₆ (37 mg, 0.22 mmol) gave 62 mg (40%) of an orange complex, [Ru^{II}(bppa)Cl]PF₆ (**3**), as single crystals.

The absorption spectrum of **3** in dichloromethane solution revealed a maximum at 437 nm ($\epsilon = 9900 \text{ M}^{-1} \text{ cm}^{-1}$) assignable to a MLCT band. The ESI-mass spectrum gave prominent peak clusters at $m/z = 625.2$ corresponding to $[\text{Ru}^{\text{II}}(\text{bppa})\text{Cl}]^+$. Anal. Calcd for **3** (C₂₈H₃₆ClF₆N₆O₂PRu): C, 43.66; H, 4.71; N, 10.91. Found: C, 43.91; H, 4.66; N, 10.82. ¹H NMR (DMSO-*d*₆): $\delta = 10.96$ (s, 1H), 9.76 (s, 1H), 8.13 (d, 1H, $J = 8.1$ Hz), 7.94 (d, 1H, $J = 4.8$ Hz), 7.87 (t, 1H, $J = 7.8$ Hz), 7.84 (d, 1H, $J = 8.1$ Hz), 7.77 (t, 1H, $J = 7.8$ Hz), 7.42 (d, 1H, $J = 8.1$ Hz), 7.41 (t, 1H, $J = 8.1$ Hz), 7.29 (t, 1H, $J = 6.9$ Hz), 7.26 (d, 1H, $J = 7.5$ Hz), 7.17 (d, 1H, $J = 7.5$ Hz), 4.81 (d, 1H, $J = 16.7$ Hz), 4.79 (d, 1H, $J = 13.4$ Hz), 4.69 (d, 1H, $J = 16.3$ Hz), 4.64 (d, 1H, $J = 13.4$ Hz), 4.26 (d, 1H, $J = 16.7$ Hz), 4.03 (d, 1H, $J = 16.3$ Hz), 1.36 (s, 9H), 1.27 (s, 9H).

[Ru^{III}(bnpa)Cl₂]PF₆ (4). To a solution of RuCl₃·3H₂O (50 mg, 0.2 mmol) in EtOH (30 mL) was added an EtOH (10 mL) solution of BNPA (89 mg, 0.19 mmol) under reflux under nitrogen atmosphere for 20 h, and then a small portion of HCl was added. After filtration and evaporation, the residue was dissolved in chloroform, to which diethyl ether was added to give a crude green precipitate, [Ru(bnpa)Cl₂]Cl. The complex was recrystallized in dichloromethane–methanol solution with coexistence of NaPF₆ (37 mg, 0.22 mmol). The isolated yield of [Ru^{III}(bnpa)Cl₂]PF₆ (**4**) was 85% (132 mg) based on the starting RuCl₃·3H₂O.

The absorption spectrum of **4** in dichloromethane solution revealed absorption maxima at 666 nm ($\epsilon = 1900 \text{ M}^{-1} \text{ cm}^{-1}$) and 328 nm ($\epsilon = 11900 \text{ M}^{-1} \text{ cm}^{-1}$) assignable to MLCT bands. The ESI-mass spectrum showed a very complicated pattern. Anal. Calcd for **4** (C₂₈H₄₀Cl₂F₆N₆PRu·0.5H₂O): C, 42.75; H, 5.25; N, 10.68. Found: C, 42.84; H, 5.06; N, 10.49.

[Ru^{II}(mppa)Cl]PF₆ (5). To a reflux solution of RuCl₃·3H₂O (50 mg, 0.2 mmol) and MPPA (75 mg, 0.19 mmol) in MeOH (30 mL) was added Et₃N (24 mg, 0.24 mmol) under nitrogen atmosphere, which was then stirred for 16 h. After addition of NaPF₆ (37 mg, 0.22 mmol), the reaction solution was filtered and then evaporated to 3 mL volume. This was allowed to stand in a refrigerator for several days to give 34 mg (25%) of orange complex, [Ru^{II}(mppa)Cl]PF₆ (**5**), as single crystals.

The absorption spectrum of **5** in dichloromethane solution exhibited MLCT bands at 649 nm ($\epsilon = 5400 \text{ M}^{-1} \text{ cm}^{-1}$) and 374 nm ($\epsilon = 4900 \text{ M}^{-1} \text{ cm}^{-1}$). The ESI-mass spectrum gave prominent peak clusters at $m/z = 526.0$ corresponding to $[\text{Ru}^{\text{II}}(\text{mppa})\text{Cl}]^+$. ¹H NMR (DMSO-*d*₆): $\delta = 11.79$ (s), 10.55 (s), 7.0–8.2 (m), 4.0–4.9 (m), 1.45 (s), 1.44 (s).

[Ru^{III}(mnpa)Cl₂]PF₆ (6). A solution of RuCl₃·3H₂O (50 mg, 0.2 mmol) in EtOH (30 mL) was refluxed under nitrogen atmosphere for 1 h to which was then slowly added an EtOH (10 mL) solution of BNPA (89 mg, 0.19 mmol). The mixed solution was refluxed under nitrogen atmosphere for 16 h, and then a small portion of HCl was added. After filtration, NaPF₆ (37 mg, 0.22 mmol) was added to the solution. This was evaporated, and the residue was dissolved in dichloromethane–MeOH. After the mixture was standing at room temperature, 55 mg (40%) of green powder precipitated. In the case of **6**, regrettably, single crystals suitable for X-ray analysis were not obtained.

The absorption spectrum of **6** in dichloromethane solution exhibited MLCT bands at 640 nm ($\epsilon = 2800 \text{ M}^{-1} \text{ cm}^{-1}$) and 341 nm ($\epsilon = 9500 \text{ M}^{-1} \text{ cm}^{-1}$). The ESI-mass spectrum gave prominent peak clusters at $m/z = 546.1$ corresponding to [Ru^{III}(mnpa)Cl₂]⁺.

[Ru^{III}(tpa)Cl₃] (8). This complex was synthesized without Et₃N in EtOH solution. A solution of RuCl₃·3H₂O (50 mg, 0.2 mmol) and TPPA (112 mg, 0.19 mmol) in EtOH (30 mL) was refluxed for 24 h. The color of the solution changed from dark brown to clear orange. After 24 h, the reaction solution was filtered and then evaporated. The crude product was dissolved in EtOH and allowed to stand in a refrigerator for several days. An orange complex, **8** (127 mg, 80%), was precipitated as single crystals suitable for X-ray analysis.

The absorption spectrum of **8** in dichloromethane solution exhibited MLCT band at 337 nm ($\epsilon = 8600 \text{ M}^{-1} \text{ cm}^{-1}$). The ESI-mass spectrum gave prominent peak clusters at $m/z = 759.2$ corresponding to [Ru^{III}(tpa)Cl₃]⁺. Anal. Calcd for **8** (C₃₃H₄₅Cl₃N₇O₃Ru): C, 50.17; H, 5.76; N, 12.02. Found: C, 49.84; H, 5.70; N, 12.02.

[Ru^{III}(tnpa)(OH)Cl]CF₃SO₃ (9). An aqueous acetone (50%) solution (30 mL) containing [Ru^{III}(tnpa)Cl₂]Cl (**2b**) (75 mg, 0.1 mmol) and AgCF₃SO₃ (30 mg, 0.12 mmol) was stirred at room temperature for 8 h. After removal of excess AgCF₃SO₃ and generated AgCl using Celite, the reaction solution was evaporated and then dissolved in dichloromethane. This solution was washed with water to remove the remaining silver salt. After evaporation, the residue was recrystallized in dichloromethane–methanol solution and 33 mg (40%) of **9** was isolated. In the crystals of **9**, there are two independent molecules in the unit cell.

The absorption spectrum of **9** in dichloromethane solution revealed absorption maxima at 627 nm ($\epsilon = 5800 \text{ M}^{-1} \text{ cm}^{-1}$) and 341 nm ($\epsilon = 12800 \text{ M}^{-1} \text{ cm}^{-1}$) assignable to MLCT bands. The ESI-mass spectrum gave prominent peak clusters at $m/z = 699.4$ corresponding to [Ru^{III}(tnpa)(OH)Cl]⁺. Anal. Calcd for **9** (C₃₄H₅₂Cl₂F₃N₇O₄SRu): C, 48.13; H, 6.18; N, 11.54. Found: C, 48.12; H, 6.28; N, 11.24.

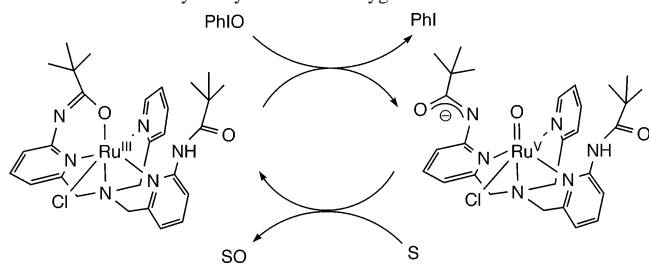
Crystal data for these complexes are summarized in Table 1, and selected bond lengths and angles are listed in Table 2.

Oxidation of Substrates. Oxidation of substrates (adamantane 68 mg, cyclooctene 55 mg, or 1-phenylethanol 66 mg (0.5 mmol)) was carried out in 1,2-dichloroethane solution (5 mL) at 40 °C in the presence of PhIO (110 mg (0.5 mmol)) and catalytic amounts of ruthenium complex (0.005 mmol) under Ar atmosphere. All other reactions for oxidation of cyclohexene and stilbenes including the experiment for the solvent effect were carried out according to the same procedure. The reaction products, which were identified by GC analysis at appropriate times, and the results of these reactions are shown in Tables 3–5 and Scheme 2.

Table 2. Selected Bond Lengths (Å) and Angles (deg)

	1	2a	3	4	5	8	9 ^a
	Ru–N(1)	2.060(3)	2.04(1)	Ru–N(1)	2.053(5)	Ru–N(1)	2.079(9)
	Ru–N(2A)	2.149(3)	2.12(1)	Ru–N(2A)	2.072(5)	Ru–N(2A)	2.10(1)
	Ru–N(2B)	2.117(3)	2.11(1)	Ru–N(2B)	2.067(5)	Ru–N(2B)	2.119(10)
	Ru–N(2C)	2.124(3)	2.12(1)	Ru–N(2C)	1.991(6)	Ru–Cl(1)	2.384(3)
	Ru–Cl(1)	2.4701(9)	2.439(4)	Ru–O(1C)	2.083(5)	Ru–Cl(2)	2.343(5)
	Ru–Cl(2)	2.439(1)	2.319(4)	Ru–Cl(1)	2.428(2)	Ru–Cl(3)	2.347(4)
	N(2A)–Ru–N(2B)	160.9(1)	N(2A)–Ru–N(2B)	N(2A)–Ru–N(2B)	163.8(2)	N(2A)–Ru–N(2B)	161.8(3)
	N(2A)–Ru–N(2C)	96.6(1)	N(2A)–Ru–N(2C)	N(2A)–Ru–N(2C)	89.6(2)	Cl(1)–Ru–N(1)	173.4(3)
	Cl(1)–Ru–N(1)	174.67(8)	Cl(1)–Ru–N(1)	O(1C)–Ru–N(1)	174.6(2)	Cl(1)–Ru–Cl(2)	84.7(1)
	Cl(2)–Ru–N(1)	95.76(9)	Cl(2)–Ru–N(1)	Cl(1)–Ru–N(1)	94.9(1)	Cl(1)–Ru–Cl(3)	89.9(1)
							Cl(1)–Ru–N(1)
							160.2(5), 161.3(5)
							84.8(4), 96.5(5)
							178.8(3), 176.9(5)
							97.1(4), 98.4(5)
							95.0(3), 95.0(4)

^a There are two independent molecules in unit cell.

Scheme 1. Catalytic Cycle for the Oxygen Transfer Reaction

Results

Synthesis and Structural Characterization of the Ruthenium Complexes with Tripodal Ligands. The tripodal ligands were synthesized according to the previously reported method.^{23,24,26} Complexation between ruthenium ion and the tripodal ligands was carried out in refluxing ethanol solution under nitrogen atmosphere in accordance with the preparation method for $[\text{Ru}(\text{tpa})\text{Cl}_2]\text{ClO}_4$ (**7a**).⁴⁸ Addition of triethylamine to the above ethanol solution gave the Ru(II) complexes.⁴⁹ Some ruthenium complexes, $[\text{Ru}(\text{tppa})\text{Cl}_2]$ (**1**), $[\text{Ru}(\text{tnpa})\text{Cl}_2]\text{ClO}_4$ (**2a**), $[\text{Ru}(\text{bppa})\text{Cl}]\text{PF}_6$ (**3**), $[\text{Ru}(\text{bnpa})\text{Cl}_2]\text{PF}_6$ (**4**), $[\text{Ru}(\text{mppa})\text{Cl}]\text{PF}_6$ (**5**), $[\text{Ru}(\text{tppa})\text{Cl}_3]$ (**8**), and $[\text{Ru}(\text{tnpa})(\text{OH})\text{Cl}]\text{CF}_3\text{SO}_3$ (**9**), were obtained as single crystals suitable for X-ray analysis, but $[\text{Ru}(\text{mnpa})\text{Cl}_2]\text{PF}_6$ (**6**) was not obtained as single crystals. Crystal data for these complexes are summarized in Table 1. Generally, TPPA, BPPA, and MPPA ligand (amide series) having 6-pivalamide groups prefer to form Ru(II) complexes as thermally stable products, while TNPA, BNPA, and MNPA ligand (amine series) having 6-neopentylamine groups gave Ru(III) complexes. The diamagnetic character of **1**, **3**, and **5** revealed that the oxidation state of the ruthenium with amide-series ligands was divalent, although the detailed structural analyses of **1** and **5** were not fully investigated because of their complicated ^1H NMR spectral patterns. The spectral pattern of **5** was unidentified, probably because some conformation isomers could be found in solution phase. The crystal structures of these complexes complete an octahedral geometry as shown in Figures 1 and 2, and selected bond lengths and angles are listed in Table 2. The configuration around ruthenium except for **8** revealed octahedral geometry consisting of one tertiary-amine nitrogen and three pyridine nitrogen atoms of the tripodal ligands and two monodentate ligands (or an amide carbonyl group) in cis-form. In comparison with the crystal structures of iron and copper complexes with the same ligands previously reported,^{22–28} octahedral geometry was ascertained for those of all Ru(II and III) complexes.

The TPPA ligand gave two kinds of ruthenium complexes, $[\text{Ru}(\text{tppa})\text{Cl}_2]$ (**1**) and $[\text{Ru}(\text{tppa})\text{Cl}_3]$ (**8**), independently in the presence or absence of triethylamine. Triethylamine, acting as a reducing reagent in ethanol solution, abstracted one chloride ion bound to ruthenium(III) to form dichlororuthenium(II) species **1**.⁵² The crystal structure of **8** showing a unique formula revealed that the ruthenium(III) ion was coordinated with three chloride ions and the two pyridine and tertiary amino nitrogen atoms of TPPA with a meridional geometry. The bond lengths between ruthenium and two chloride ions in **2a** with TNPA ligand were 2.319(8) and

2.439(7) Å, respectively, in which the chloride ion ($\text{Cl}(2)$) with the shorter bond length occupied the cis position to the tertiary-amine nitrogen ($\text{N}(1)$) of TNPA and the longer one ($\text{Cl}(1)$) occupied the trans position. In **4** with BNPA ligand, such a difference between the bond lengths of two chloride ligands was also observed (Table 2). Since those in other complexes with tripodal ligands, such as TPA⁴⁸ or TEPA (tris(2-pyridylethyl)amine),¹⁹ were approximately equal, such a difference in **2** or **4** was caused by the coordination of TNPA or BNPA. This effect is interpreted in terms of a hydrogen-bonding interaction between the chloride ligand and the NH groups of TNPA or BNPA.^{25,26} The chloride ion with an elongated bond of $\text{Ru}-\text{Cl}(1)$ in **2** was easily substituted by hydroxide ligand in the presence of AgNO_3 in aqueous acetone solution to give the $\text{Ru}-\text{OH}$ complex, $[\text{Ru}(\text{tnpa})(\text{OH})\text{Cl}]^+$ (**9**). The $\text{Ru}-\text{O}$ bond lengths in **9** (2.015(9) and 2.01(1) Å) were similar to those of the other ruthenium complexes previously reported.¹⁹ In the crystal of **9**, the interatomic distances between three amine-nitrogen atoms of 6-neopentylamino group ($\text{N}(3\text{A})$, $\text{N}(3\text{B})$, and $\text{N}(3\text{C})$) and the hydroxo oxygen atom ($\text{O}(1)$) were 2.71–2.88 Å, which were within hydrogen-bonding distance (2.5–3.2 Å).⁴⁷ From these findings, amine and amide groups at the pyridine 6-position of tripodal pyridylmethylamine ligands (TPPA, BPPA, MPPA, TNPA, BNPA, and MNPA) can play a hydrogen-bonding interaction role around the metal center to stabilize the coordination of the monodentate axial ligand.^{25,26,53–55}

Structural Description of 3 and 4 as Typical Ruthenium Complexes. The structures of **3** and **4** representative of the ruthenium complexes employed here were confirmed on the basis of absorption, IR, NMR, and mass spectra and elemental analysis as well as the X-ray diffraction method. The orange complex **3** (Figure 1b) completed an axially compressed octahedral structure which was coordinated with three pyridine nitrogen atoms, one tertiary amine nitrogen atom, one pivalamide carbonyl oxygen atom, and one chloride ion. Since carbonyl oxygen of one pivalamide moiety coordinates to ruthenium in **3**, the BPPA ligand acts as a pentadentate ligand. The presence of one counterion in the crystal as well as the diamagnetic character indicates that the oxidation state of the ruthenium in **3** is divalent. The positive ion ESI-mass spectrum of **3** gave peak clusters at $m/z = 625.2$ corresponding to $[\text{Ru}^{\text{II}}(\text{bppa})\text{Cl}]^+$ ion. The electronic absorption spectrum of **3** in dichloromethane solution exhibited an MLCT band assignable to a $d \rightarrow \pi^*$ transition at 437 nm ($\epsilon = 9900 \text{ M}^{-1} \text{ cm}^{-1}$).⁵⁶ The IR spectrum of **3** showed two $\text{C}=\text{O}$ stretching vibration bands of amide group at 1629 and 1695 cm^{-1} . In the ^1H NMR spectrum of **3** in $\text{DMSO}-d_6$ solution, two amide protons were

(52) Gerli, A.; Reedijk, J.; Lakin, M. T.; Spek, A. L. *Inorg. Chem.* **1995**, *34*, 1836.

(53) Jitsukawa, K.; Harata, M.; Arai, H.; Sakurai, H.; Masuda, H. *Inorg. Chim. Acta* **2001**, *324*, 108.

(54) Yamaguchi, S.; Tokairin, I.; Wakita, Y.; Funahashi, Y.; Jitsukawa, K.; Masuda, H. *Chem. Lett.* **2003**, *32*, 406.

(55) Yamaguchi, S.; Wada, A.; Funahashi, Y.; Nagatomo, S.; Kitagawa, T.; Jitsukawa, K.; Masuda, H. *Eur. J. Inorg. Chem.* **2003**, 4378.

(56) Chakraborty, S.; Walawalkar, M. G.; Lahiri, G. K. *J. Chem. Soc., Dalton Trans.* **2000**, 2875.

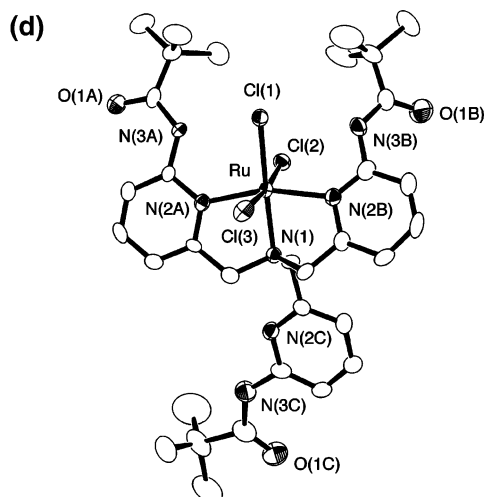
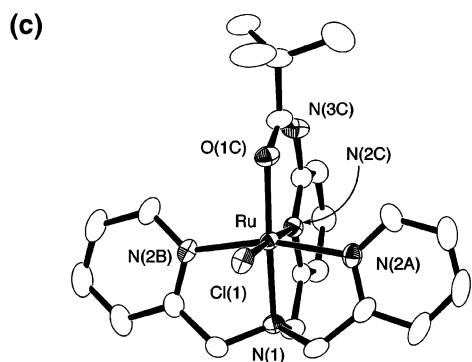
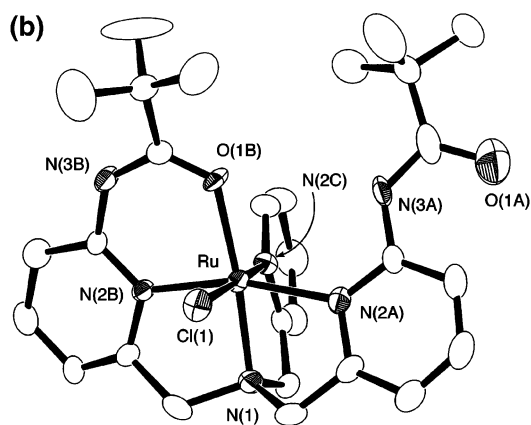
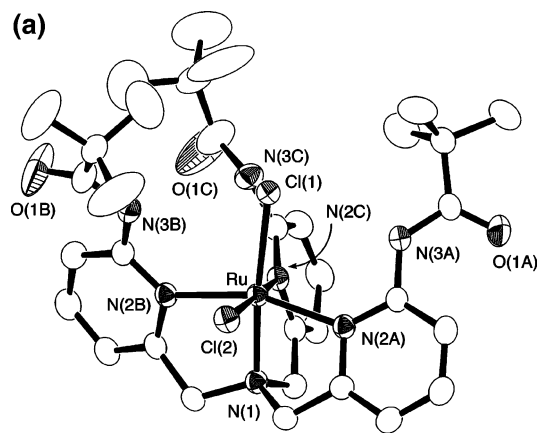


Figure 1. Crystal structures of the amide-series complexes: (a) $[\text{Ru}^{\text{II}}(\text{tppa})\text{Cl}_2]$ (**1**); (b) $[\text{Ru}^{\text{II}}(\text{bppa})\text{Cl}]^+$ (**3**); (c) $[\text{Ru}^{\text{III}}(\text{mppa})\text{Cl}]^+$ (**5**); (d) $[\text{Ru}^{\text{III}}(\text{tppa})\text{Cl}_3]$ (**8**).

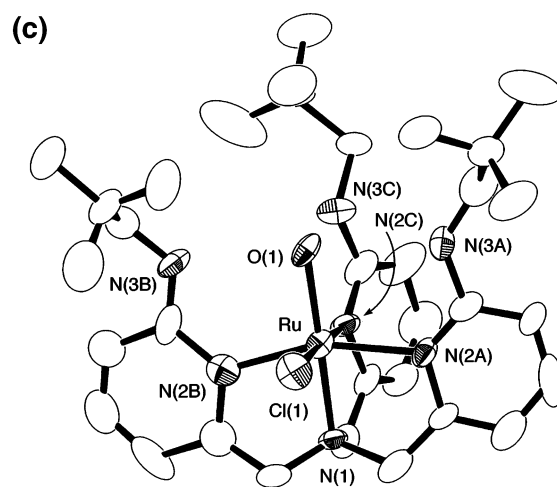
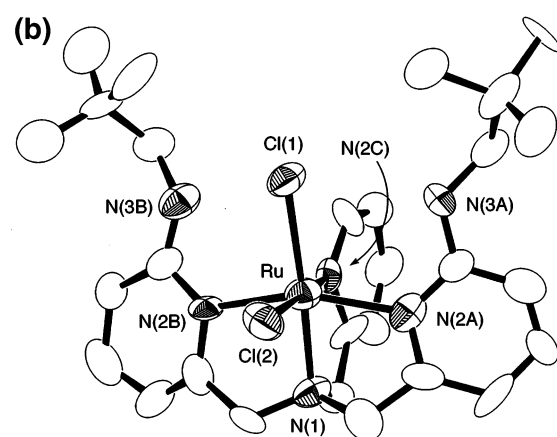
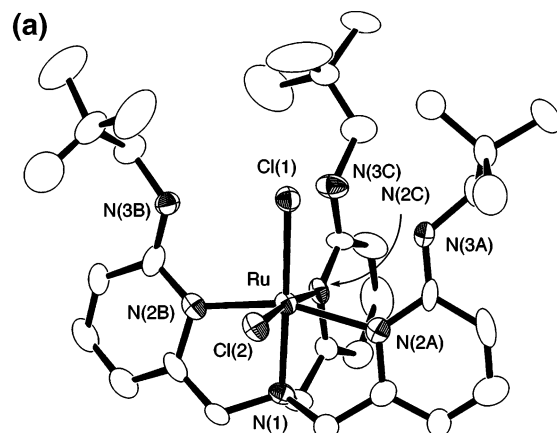


Figure 2. Crystal structures of the amine-series complexes: (a) $[\text{Ru}^{\text{III}}(\text{tpa})\text{Cl}_2]^+$ (**2**); (b) $[\text{Ru}^{\text{III}}(\text{bnpa})\text{Cl}_2]^+$ (**4**); (c) $[\text{Ru}^{\text{III}}(\text{tpa})(\text{OH})\text{Cl}]^+$ (**9**).

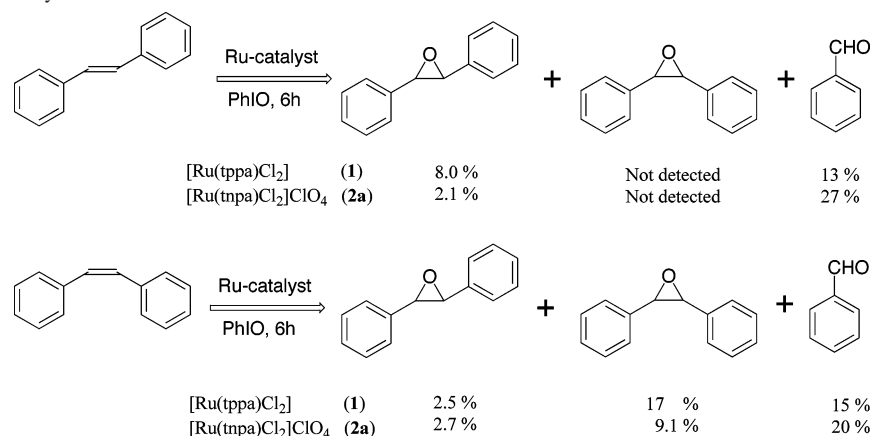
observed at 10.96 and 9.76 ppm, and two tertiary butyl groups were at 1.36 and 1.27 ppm, respectively. Moreover, three kinds of pyridine ring patterns were observed in the aromatic region. Two pyridine rings having 6-pivalamide group of BPPA were unequivalent in their coordination modes. Accordingly in the solution phase of **3**, two kinds of the carbonyl groups attached to BPPA were observed which was also the case in the crystal.

As reported previously, active species of the ruthenium-catalyzed oxygen transfer reaction were high-valent $\text{Ru}=\text{O}$ intermediates.⁴⁰ In the positive ESI-mass spectrum, the active

Table 3. Catalytic Activity for Hydroxylation of Adamantane and Epoxidation of Cyclooctene by Various Ruthenium Complexes (1–7)^a

complex	adamantane					cyclooctene		
	TON ^b					TON ^c		
	1-ol ^d	2-ol ^d	2-one ^d	1-Cl ^d	2-Cl ^d	selectivity ^e	1 h	8 h
[Ru(tppa)Cl ₂] (1)	8	0.7	0.4	0.4	0.4	17	11	27
[Ru(bppa)Cl]PF ₆ (3)	9	0.4	0.7	0.8	0.4	27	12	29
[Ru(mppa)Cl]PF ₆ (5)	10	0.2	0.5	0.7	0.3	42	19	39
[Ru(tpa)Cl ₂]PF ₆ (2)	17	0.4	1.2	0.4	0.2	32	4	17
[Ru(bnpa)Cl ₂]PF ₆ (4)	22	trace	1.1	0.5	0.2	59	11	35
[Ru(mnpa)Cl ₂]PF ₆ (6)	28	0.2	1.2	0.5	0.3	61	20	42
[Ru(tpa)Cl ₂]PF ₆ (7)	8	0.1	0.4	0.3	0.2	47	19	50

^a Reaction conditions: substrate (0.5 mmol), PhIO (0.5 mmol), ruthenium complex (0.005 mmol), 1,2-dichloroethane (5 mL); 40 °C under Ar, 60 min. ^b TON (turnover numbers) were determined on the basis of the product yields estimated by GC analysis at 60 min. ^c TON for the formation of 1,2-epoxycyclooctane was determined by GC analysis at 1 and 8 h. ^d Abbreviations: 1-ol = 1-adamantanol; 2-ol = 2-adamantanol; 2-one = 2-adamantanone; 1-Cl = 1-chloroadamantane; 2-Cl = 2-chloroadamantane. ^e Selectivity for oxidation of the tertiary or secondary C–H bond on the oxidation of adamantane was defined by the following equation: $[1\text{-ol}]/([2\text{-ol}] + [2\text{-one}])$.

Scheme 2. Ruthenium-Catalyzed Oxidation of Stilbenes

species generated from **3** and PhIO in the dichloromethane gave prominent peak clusters at m/z 624.2 and 640.2, corresponding to the $[\text{Ru}^{\text{III}}(\text{bppa}^-)\text{Cl}]^+$ and $[\text{Ru}^{\text{V}}(\text{bppa}^-)(\text{O})\text{Cl}]^+$ ions, respectively (bppa[−] is the monodeprotonated form at the amide NH of the coordination form of BPPA). These findings indicate that carbonyl oxygen atom of the 6-pivalamide group coordinating to ruthenium in **3** might be substituted by the oxo species, when an oxidant is used. On the other hand, the reaction of **4** and PhIO did not show such peak clusters assignable to Ru=O. Self-oxidation of BNPA occurred on **4** to give a complicated fragment pattern in measurement of the mass spectrum with coexistence of PhIO.

The crystal structure of **4** in Figure 2b completed an axially compressed octahedron with coordination of four nitrogen atoms of BNPA and two chloride ions. The electronic absorption spectrum of the green complex **4** in dichloromethane solution gave two MLCT bands at 666 nm ($\epsilon = 1900 \text{ M}^{-1} \text{ cm}^{-1}$) and 328 nm ($\epsilon = 12000 \text{ M}^{-1} \text{ cm}^{-1}$). Judging from the paramagnetic property and the presence of one counterion in the crystal, the oxidation state of the ruthenium in **4** is trivalent.

Reactivity of Ruthenium–Oxo Species. All the ruthenium complexes (**1–7**) showed catalytic activity for epoxidation of olefins, hydroxylation of alkanes, and dehydrogenation of alcohols in the presence of PhIO under anaerobic conditions, although the yields of the oxidation products were relatively low on account of using substitutionally inert

chloride ligand.⁵⁷ Epoxidation of cyclooctene catalyzed by the complex **3** in 1,2-dichloroethane solution at 40 °C for 8 h gave 29% yield of 1,2-epoxycyclooctane, and a 39% yield of epoxide was obtained even if less hindered **5** was used as a catalyst (Table 3). The relatively lower reactivity compared with the case of periodate oxidant is interpreted by the oxidation ability of PhIO.⁵⁸ In the case of ^tBuOOH as an oxidant, the yield of the corresponding epoxide was only 4.7%. Since MCPBA (*m*-chloroperbenzoic acid), which is often used to generate metal–oxo species, is known to promote epoxidation of olefins, hydroxylation of adamantane, and Baeyer–Villiger oxidation of ketones,⁵⁹ it is not utilized for our oxidation experiments to avoid further complicated reactions. Because of easy handling we chose PhIO as an efficient oxidant for ruthenium-catalyzed oxidations to investigate the correlation of the structural diversity of the complexes and the catalytic activities. Active species of the ruthenium complexes for oxygen transfer reaction are considered as high-valent Ru(V)=O species as reported previously.⁴⁰ As shown in Scheme 1, the two electron oxidation process by PhIO in the Ru(III) and Ru(V)=O redox cycle is considered for oxygen transfer reactions.

The tertiary hydrogen in adamantane was easily abstracted by the Ru=O species in comparison with the secondary one

(57) Barf, G. A.; Sheldon, R. A. *J. Mol. Catal. A: Chem.* **1995**, *102*, 23.

(58) Bailey, A. J.; Griffith, W. P.; Savage, P. D. *J. Chem. Soc., Dalton Trans.* **1995**, 3537.

(59) Renz, M.; Meunier, B. *Eur. J. Org. Chem.* **1999**, 737.

Table 4. Solvent Effect for Hydroxylation of Adamantane Catalyzed by the Ruthenium Complex **4**^a

solvent	TON ^b				
	1-ol ^c	2-ol ^c	2-one ^c	1-Cl ^c	2-Cl ^c
1,2-dichloroethane	22	trace	1.1	0.5	0.2
CH ₂ Cl ₂	16	0.4	1.0	0.4	0.3
CHCl ₃	22	0.2	0.3	5.0	1.5
CCl ₄	1.5	0.1	nd ^d	5.8	1.2
CH ₃ CN	0.4	0.2	nd ^d	nd ^d	nd ^d
C ₂ H ₅ CN	0.5	0.3	nd ^d	trace	0.2

^a Reaction conditions: adamantane (0.5 mmol), PhIO (0.5 mmol), ruthenium complex (0.005 mmol), solvent (5 mL); 40 °C under Ar, 60 min. ^{b,c} TON and abbreviations are the same as in Table 3. ^d nd: not detected.

to give 1-adamantanol, so that the yield of 1-adamantanol surpassed total amounts of 2-adamantanol and 2-adamantanone. Since the Ru=O species also had the oxidation ability of secondary alcohols to ketones,^{60,61} 2-adamantanol was further oxidized to 2-adamantanone. To examine the catalytic activity for the dehydrogenation of alcohols, oxidation of 1-phenylethanol catalyzed by these ruthenium complexes was carried out in the presence of PhIO in dichloromethane solution at 40 °C. At 60 min, acetophenone was obtained as a sole product in 25% yield for **1**, 42% for **2**, 49% for **3**, 42% for **4**, 30% for **5**, and 57% for **6**, respectively. In the reaction performed with **3**, moreover, the yield of acetophenone reached 70% when the reaction time was extended to 3 h. Therefore, selectivity in Table 3 was defined for oxidation of tertiary C–H vs the secondary one.

In the cases of the amine-series complexes, **2**, **4**, and **6**, their oxidation activities for adamantane were relatively high in comparison with those in the amide-series complexes, **1**, **3**, and **5**, as shown in Table 3, where [Ru(tpa)Cl₂]₂PF₆ (**7**), bearing no substituent at the pyridine 6-position, was used as a reference compound. The catalytic activity for hydroxylation of adamantane is affected by the nature of the substituent groups of the ligands and by the steric bulkiness around the metal center in the complex. The complexes **3–6**, containing bis- and monosubstituted groups at the pyridine 6-position, gave relatively large amounts of 1-adamantanol in comparison with **1** and **2** containing trisubstituted groups. Decreasing of steric bulkiness around metal center of the complexes accelerates hydroxylation activity, which is interpreted in terms of the easy approach of oxidant or substrate to the metal center during the catalytic cycle.

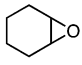
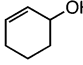
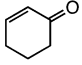
Formation of 1- and 2-chloroadamantanes indicates that a radical intermediate is generated in this reaction condition.⁶² To understand such chlorination, the solvent effect was investigated using complex **4** as a catalyst. As shown in Table 4, the hydroxylation activity in halogenohydrocarbon solvent is superior to that in nitrile one, and chloroadamantanes are formed in the former solvent. In carbon tetrachloride, especially, total amounts of the oxygenation products were less than the sum of 1- and 2-chloroadamantanes. Formation

(60) Marko, I. E.; Giles, P. G.; Tsukazaki, M.; Chelle-Regnaut, I.; Urch, C. J.; Brown, S. M. *J. Am. Chem. Soc.* **1997**, *119*, 12661.

(61) Che, C.-M.; Cheng, K.-W.; Chan, M. C. W.; Lau, T.-C.; Mak, C.-K. *J. Org. Chem.* **2000**, *65*, 7996.

(62) Bravo, A.; Fontana, F.; Minisci, F.; Serri, A. *J. Chem. Soc., Chem. Commun.* **1996**, 1843.

Table 5. Oxidation of Cyclohexene Catalyzed by the Complexes **3** and **4**^d

Complexes	Products (yield %)			E/A ^c
				
[Ru(bppa)Cl]PF ₆ (3) ^a	46	0.7	1.5	21
(3) ^b	16	1.3	1.9	5.2
[Ru(bnpa)Cl ₂]PF ₆ (4) ^a	20	0.6	2.6	6.3
(4) ^b	4.2	1.3	2.2	1.2

^a In 1,2-dichloroethane. ^b In acetonitrile. ^c E/A = epoxidation/allylic oxidation (1,2-epoxycyclohexane/(2-cyclohexen-1-ol + 2-cyclohexen-1-one)). ^d Reaction conditions: cyclohexene (0.5 mmol), PhIO (0.5 mmol), ruthenium complex (0.005 mmol), solvent (5 mL); 40 °C under Ar, 4 h.

of small amount of 2-chloroadamantane in propionitrile is explained by the reaction derived from chloride ion bound to **4**. The yields of 1- and 2-chloroadamantanes increased at higher temperature in 1,2-dichloroethane. Since the radical reaction is known to be accelerated in halogenohydrocarbons,⁶³ this reaction involves a radical intermediate.

Reactivity for Epoxidation and Allylic Oxidation of Cyclohexene. Oxidation of cyclohexene catalyzed by the complex **3** gave 1,2-epoxycyclohexane in 46% yield, accompanied with small amounts of allylic oxidation products (2-cyclohexen-1-ol (0.7%) and 2-cyclohexen-1-one (1.5%)) as summarized in Table 5.⁴⁰ Under this reaction condition allylic alcohol was furthermore oxidized to give α,β -unsaturated ketone through ruthenium-catalyzed oxidative dehydrogenation pathway. 2-Cyclohexen-1-one was obtained through two reaction pathways, such as direct formation from cyclohexene through abstraction of allylic proton by the metal-oxo intermediate and two-step reaction via 2-cyclohexen-1-ol. The ratio (E/A) of epoxidation to allylic oxidation (sum of 2-cyclohexen-1-ol and 2-cyclohexen-1-one) catalyzed by **3** was 21 in 1,2-dichloroethane solution. In acetonitrile solution, however, the selectivity and reactivity for epoxidation decreased. Such solvent effect indicates that a radical intermediate is involved in the reaction as well as in the case in Table 4.^{4,63} The reaction catalyzed by **4** gave only 20% yield of 1,2-epoxycyclohexane, accompanied with 2-cyclohexen-1-ol (0.6%) and 2-cyclohexen-1-one (2.6%), in which the E/A value was 6.3. In comparison with the catalytic activity of **3**, notably, that of **4** for allylic oxidation increased and that for epoxidation decreased. In the case of the [Ru^{IV}(bpy)₂(py)(O)] complex, Mayer et al. reported some interesting findings: The ratio of 2-cyclohexen-1-ol to 2-cyclohexen-1-one increased when excess amounts of cyclohexene were employed,⁶⁴ and hydrogen atom abstraction was the dominant mechanism for C–H bond activation of alkylaromatic compounds.⁶⁵ Moreover, this complex as a Ru(IV)=O species showed very low epoxidation activity for α -methylstyrene. Judging from a different oxidation activity as mentioned above, the active species derived from these ruthenium complexes (**1–6**) with tripodal ligands and PhIO is not Ru(IV)=O.

(63) Mayo, F. R. *Acc. Chem. Res.* **1968**, *1*, 193.

(64) Stultz, L. K.; Huynh, M. H. V.; Binstead, R. A.; Curry, M.; Meyer, T. J. *J. Am. Chem. Soc.* **2000**, *122*, 5984.

(65) Bryant, J. M.; Matsuo, T.; Mayer, J. M. *Inorg. Chem.* **2004**, *43*, 1587.

Reactivity for Epoxidation and Cleavage of *cis*- and *trans*-Stilbenes. Oxidation of *trans*-stilbene catalyzed by **1** or **2** gave benzaldehyde as a main product and *trans*-stilbene oxide as a sole product for epoxidation without formation of the *cis* one (Scheme 2). In this case, the yield of the *trans*-stilbene oxide was low in comparison with the case of *cis*-stilbene. The oxidation of *cis*-stilbene catalyzed by **1** at 25 °C for 6 h gave *cis*-stilbene oxide in 17% yield, accompanied with *trans*-stilbene oxide (2.5%) and benzaldehyde (15%). At 70 °C, the yield of *cis*-stilbene oxide was 14% and that of benzaldehyde was 36%. The epoxidation activity of **1** is relatively higher than that of **2**, but the cleavage reaction in **2** proceeds more smoothly than that in **1**, indicating that the active species mediated by **1** or **2** are slightly different from each other. Two kinds of species, such as Ru(V)=O and Ru(IV)-O• ones, have been proposed as active species in these reactions.⁴² The C=C bond cleavage reactions are well-known in the oxidation catalyzed by the high-valent ruthenium-oxo species.¹³ For example, oxidation of stilbenes catalyzed by the RuCl₃-Oxone-NaHCO₃ system in aqueous CH₃CN solution gave a high yield of benzaldehyde, where epoxide and diol were often accompanied.⁶⁶ Obviously in Scheme 2, oxidation activity for *cis*-stilbene is superior to that for *trans*-one, which is interpreted by the steric factor of the tris-substituted tripodal ligands. Approach of the more bulky *trans*-stilbene to the active species of the complex might be hard in comparison with the *cis* one, so that the yield of epoxide decreased.⁶⁷ Notably, formation of *trans*-stilbene oxide from *cis*-stilbene indicates that the radical intermediate through the rotation of carbon-carbon single bond affords the thermally stable *trans* one.^{3,4,39}

Discussion

The epoxidation activities of the amide-series complexes, **1**, **3**, and **5**, are relatively high in comparison with those of amine-series complexes, **2**, **4**, and **6**. However, for hydroxylation of adamantane, allylic oxidation of cyclohexene, and cleavage of stilbene, the amine ones showed higher reactivity than the amide ones. Amide and amine groups substituted at the pyridine 6-position of the tripodal ligands, which affect the character of the active species, are classified as electron-withdrawing and electron-donating ones, respectively.^{43,44} In the ruthenium-catalyzed oxygen transfer reaction, generally, a high-valent Ru=O species (Ru(IV), Ru(V), or Ru(VI)) has been considered as an active species.^{12-14,68} The characteristic absorption bands of Ru=O species with nitrogen-containing ligands are known to be observed about 380–400 nm.^{33,69} In our investigation, Ru(V)=O has been considered as an active species, which was suggested by the ESI-mass spectrum,⁴⁰ although the typical absorption spectrum was not observed during the reaction because of overlapping with a very large absorption due to a π - π^* transition of pyridine ligands.

Table 6. Summarized Reactivity for the Ruthenium Complexes with Tripodal Ligands

reactivity	amide-series complexes 1 , 3 , and 5	amine-series complexes 2 , 4 , and 6
epoxidation of olefins (cyclooctene, cyclohexene, <i>cis</i> - and <i>trans</i> -stilbene)	high	low
hydroxylation of alkane (adamantane)	low	high
allylic oxidation of olefin (cyclohexene)	low	high
cleavage reaction of olefins (<i>cis</i> - and <i>trans</i> -stilbene)	low	high
position of oxo ligand occupied	trans-N to tertiary amine	cis-N to tertiary amine
preferential character of Ru-oxo species	Ru(V)=O	Ru(IV)-O•

The mechanistic investigations on oxidation of aromatic alkenes by monooxo Ru(IV)=O complexes³⁷ and epoxidation of alkenes by *trans*-dioxo O=Ru(VI)=O porphyrins were carried out by Che et al.,³⁹ in which several oxidation pathways, such as concerted oxene insertion, metallaoxetane formation, alkene-derived cation radical, carbocation, and carboradical, were considered from the kinetic data. The possibility of a radical intermediate has been also discussed because of the formation of a charge-transfer complex of alkene and metal-oxo species.^{37,39} Recently, Meyer et al. reported that the Ru(IV)=O species attacks the C-H bond rather than olefin double bond,⁶⁴ probably indicating that the lower valent metal-oxo species had radical character. These are consistent with our previous report that the oxidation activity of the ruthenium complexes [Ru(babp)(dmsO)(Y)] with square planar ligand BABP (H₂BABP = 6,6'-bis-(benzoylamino)-2,2'-bipyridine) has been controlled by the axial ligand Y.⁴² In BABP complexes, epoxidation activity for cyclohexene was high but allylic oxidation activity was low when the electron-donating imidazole was used as Y, whereas the opposite phenomena were observed when pyridine was used. Obviously, the axial ligand coordinated at the *trans* position of the metal-oxo species causes a *trans* influence for the reactivity. From the results indicated in the case of the [Ru(babp)(O)(Y)] catalyst, we can consider that the reactivity of Ru(V)=O species in **1**–**6** matches well with the *trans* influence as follows. The oxo species bound to the *trans* position of the tertiary amine of the tripodal ligand is mainly affected by the electron-donating tertiary amine (Chart 1, left), while another one bound to the *cis* position of the tertiary amine is affected by pyridine (Chart 1, right).

The complementary reactivities as summarized in Table 6 indicate that the Ru=O species employed here are classified into two types. The catalytic intermediate in these reactions might be interpreted in terms of contribution of character from both Ru(V)=O and Ru(IV)-O•, which are electronically equivalent to each other and generated dependently by the *trans* influence of the coordinating nitrogen atoms, such as amine-nitrogen or pyridine-nitrogen.⁷⁰ The oxidation activities catalyzed by the high-valent ruthenium

(66) Yang D.; Zhang, C. *J. Org. Chem.* **2001**, *66*, 4814.

(67) Natarajan, A.; Madalengoitia, J. S. *Tetrahedron Lett.* **2000**, *41*, 5789.

(68) Taqui Khan, M. M.; Chatterjee, D.; Merchant, R. R.; Paul, P.; Abdi, S. H. R.; Srinivas, D.; Siddiqui, M. R. H.; Moiz, M. A.; Bhadbhade, M. M.; Venkatasubramanian, K. *Inorg. Chem.* **1992**, *31*, 2711.

(69) Che, C.-M.; Li, C.-K.; Tang, W.-T.; Yu, W.-Y. *J. Chem. Soc., Dalton Trans.* **1992**, 3153.

(70) Bernadou, J.; Meunier, B. *Chem. Commun.* **1998**, 2167.

Ruthenium Complexes with Tripodal Ligands

complexes with tripodal ligands are also controlled by the steric factor around the metal center, where easy approach of oxidant or substrate to metal center is important for the reactivity.

Conclusion

Ruthenium complexes with tripodal tris(pyridylmethyl)-amine ligands bearing pivalamide and neopentylamine groups at the pyridine 6-position have been prepared and structurally characterized. All ruthenium complexes employed here completed an octahedral geometry. In the oxidation of various substrates catalyzed by them and PhIO oxidant, epoxidation activities of the amide-series complexes are relatively high in comparison with those of amine-series complexes. On the other hand, for C–H bond activation and C=C bond cleavage reaction, the amine ones showed higher reactivity than the amide ones. Such complementary reactivities of the complexes have been regulated by the

electronic and/or the steric characters of the substituent at the pyridine 6-position of the ruthenium complexes. In these ruthenium-catalyzed oxygen transfer reactions, the Ru(V)=O species is considered as an active species, of which reactivity in **1–6** matches well with the trans influence caused by the tertiary amine or pyridine of the tripodal ligands.

Acknowledgment. This work was supported partly by a Grant-in-Aid for Scientific Research from the Ministry of Education, Science, Sports, and Culture of Japan and supported in part by a grant from the NITECH 21st Century COE Program to which our thanks are due.

Supporting Information Available: X-ray crystallographic files in CIF format for complexes **1–5**, **8**, and **9**. This material is available free of charge via the Internet at <http://pubs.acs.org>.

IC0494399